Electron energy loss spectroscopy of core-electron excitation in anisotropic systems: Magic angle, magic orientation, and dichroism

Y. Sun and J. Yuan*
Department Materials Science and Engineering, Tsinghua University, Beijing, China
(Received 16 January 2004; revised manuscript received 27 September 2004; published 16 March 2005)

A general theory for the detection of the core-level electronic excitation in anisotropic systems using angular integrated electron energy-loss spectroscopy (EELS) has been presented. Magic angle conditions, at which spectra are independent of specimen orientation, are proved to be valid for all anisotropic systems. Discrepancies in the magic angle determination are thoroughly investigated from the theoretical point of view. The magic angle electron energy loss spectroscopy (MAEELS) can be directly interpreted as spherical averaged spectroscopy. From the explicit expression for the EELS cross section for all the anisotropic systems, a magic specimen orientation is also found to exist in certain low symmetry systems, where spectra acquired are also equivalent to the fully orientationally averaged spectra. Our analysis provides a useful guide for the experimental determination of electronic structure information in anisotropic systems, including their dichroic signals.

DOI: 10.1103/PhysRevB.71.125109 PACS number(s): 79.20.Uv, 03.65.Nk, 34.80.Dp, 71.15.Ap

I. INTRODUCTION

Anisotropic systems differ from isotropic ones in that their response to an applied force or field depends not only on the magnitude but also on the orientation of these influences.[1] For electron energy loss spectroscopy (EELS) or x-ray absorption spectroscopy (XAS), a good example is the carbon 1*s* core electron excitation in graphite.[2–7] Excitation into the unoccupied states of π symmetry is only allowed if the applied field is along the direction normal to the graphite sheet (defined to be the local *z* axis). Excitation into the unoccupied states of σ symmetry can only occur if the applied field lies in the plane of the graphite sheet (defined to be the local *x*-*y* plane). As a consequence, the intensities of these two excitations depend on the specimen orientation in general. Concerning electronic excitation, many important systems show anisotropy such as familiar layered materials like graphite and BN,[8] non-central symmetric semiconducting compounds such as GaN,[9] superconductors such as YBaCuO (Refs. 10–14) and MgB_2.[15–18] Some nanostructures such as nanotubes and nanoonions can be considered as roll-up versions of layered materials, so the local anisotropy also changes with the spatial location of the probe.[19,20] In addition, shape or local field effects may turn an isotropic transition into an anisotropic one.[21]

Anisotropic response is a gift to the experimentalists as it offers further insight into the electronic excitation process. It can also be used to determine the local orientation of the anisotropic materials[22,23] or their internal magnetic field.[24] In this paper, we focus on the complexity anisotropy brings to EELS measurements, which now also depend on the precise orientation of the specimen. In EELS, the applied field responsible for electronic excitation is parallel to the direction of the momentum transfer vector **q** of the incident electron in the inelastic scattering.[25] As shown in Fig. 1, by virtue of momentum conservation, both the magnitude and the direction of the vector **q** are functions of the electron scattering angle θ.

In the angular integrated spectroscopy with a centered circular detector, a standard experimental condition particularly useful for achieving high spatial resolution and high signal to noise ratio,[14] excitations induced by the applied fields are summed over a range of **q** directions.[26–28] There exists a number of theoretical investigation of the partially angular integrated EELS cross section as a function of the beam convergence angle and the detector collection angle as well as a function of the specimen orientation, but usually only for the simplest uniaxial system.[19,26–31] Among them, Menon and Yuan[28] showed both experimentally and theoretically that there exists a magic angle (MA) at which the EELS fine structure is independent of the specimen orientation. Study of EELS fine structure at such magic angle conditions may be called magic angle electron energy loss spectroscopy (MAEELS). This is very important for nano-scale EELS analysis as the variation observed in MAEELS can be directly interpreted in terms of the variation in the underlying

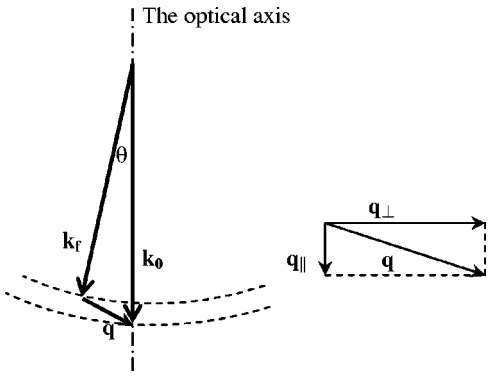

FIG. 1. In an inelastic scattering, the momentum transfer vector **q** is determined by the initial and final wave-vector $\mathbf{k}_0$ and $\mathbf{k}_f$. The angle between the two wave vectors is defined as the scattering angle θ. In the parallel illumination case, θ always equals β defined as the angle between the wave vector of scattering electrons $\mathbf{k}_f$ and the optical axis.

electronic excitations. Their work predicts the magic angle for a parallel beam illumination ($MA_{\|}$) is $4\theta_E$, where θ_E is the characteristic angle and has an approximate form $\theta_E = E/2E_0$ (the more accurate definition is given by Ritchie and Howie[32]), with E being the energy-loss and E_0 the energy of incident fast electrons. There have been many different derivations for magic angle conditions, however, there is still a controversy as to its precise values.[10,19,26–29,33] It is also not sure whether MAEELS at different magic angle conditions are equivalent, or whether the physical meaning of MAEELS is well understood. In addition, the existence of magic angle condition in other lower symmetry systems has not been properly investigated. Therefore, a detailed and general analysis of the core-level EELS in anisotropic systems is required.

The paper is organized as follows. In Sec. II, we present a thorough analysis of core-level EELS cross section in anisotropic systems and we derive a definition for magic angle conditions valid for all anisotropic systems. In Sec. III, we show that the spectral information obtained at the magic angle is equivalent to orientationally averaged spectra. We also investigated the different approaches for magic angle conditions analysis reported in the literature and showed that they were all based on the same theoretical assumptions. The reasons for the discrepancies in magic angle values are investigated. In Sec. IV, we concentrated on analyzing the EELS cross sections for more commonly encountered orthogonal systems. We found there is a so-called "magic orientation" in which the spectral fine structure is also equivalent to the rotationally averaged spectra. The relationship between these MAEELS and other more established forms of magic angle spectroscopies such as XAS and magic angle spinning nuclear magnetic resonance (MAS-NMR) is discussed. By expressing the cross section in terms of MAEELS and the remaining dichroic signals, we also provide experimentalists with a new prospect for the study of dichroism in anisotropic systems.

II. GENERALIZED THEORY

There are two ways to study the electronic excitation cross section in anisotropic systems: the macroscopic approach is to use the dielectric function and the microscopic approach is to calculate directly the quantum mechanical transition matrix element. Both approaches have been reported in the literature of the analysis of anisotropic EELS (Refs. 10, 19, 26, 27, 29, 33, and 34) and physically they should yield the same result. To facilitate comparison of these reports, we will also make our derivation using both approaches. It is known that the quantum mechanical approach can reveal the microscopic physics involved, but because of the need for accurate wave functions, it does not always yield useful experimental results. On the other hand, the dielectric approach is a phenomenological description of materials response that can be measured accurately, even though the microscopic origin of the electronic transitions may be obscured.[21]

A. Dielectric formalism

Here we start with the dielectric approach where the calculation is relatively straightforward, because the information required is not the detailed form of excitation but the overall effect in terms of the response to a perturbation described by[35]

$$D_i = \sum_j \varepsilon_0 \varepsilon^{ij} E_j, \tag{1}$$

where **D**, the electric displacement, is related to the electric field **E** by the well-known ε^{ij} the dielectric function of the material system. ε^{ij} is a "metric tensor," (Ref. 36), defined in terms of a reference frame where the orthogonal principal axes are aligned with the major symmetry directions of the physical system. For convenience, we have defined this reference frame as the sample frame (x,y,z).

The imaginary part of $(-1/\varepsilon)$ is known as the energy-loss function.[25–28] It provides a complete description of the response of the medium through which the fast electron is traveling. The double differential cross section used to estimate the intensity of EELS in an anisotropic system can be expressed as:[25,27]

$$\frac{d\sigma^2(\mathbf{q})}{dEd\Omega} = \frac{4m_e}{na_0h^2}\,\mathrm{Im}\left(-\frac{1}{\sum_{i,j} q_i \varepsilon^{ij} q_j}\right), \tag{2}$$

where m_e is the mass of the fast electron and **q** the momentum transfer vector of the fast electrons in the inelastic scattering process (see Fig. 1), n the number of atoms per unit volume of the material, a_0 the Bohr atomic radius, h the Plank constant, q_i and q_j the projection of **q** in the sample frame. Note that the components of the dielectric function are assumed not to be a function of **q**, and this assumption corresponds to the dipole approximation in the quantum mechanical analysis of single electron transitions.[35]

We will restrict our discussion to core electron excitations in which we use the approximation[25–27] for $\varepsilon_1 = \mathrm{Re}(\varepsilon)$ and $\varepsilon_2 = \mathrm{Im}(\varepsilon)$, $\varepsilon_1 \approx 1$ and $\varepsilon_2 \approx 0$. Equation (2) can then be simplified to

$$\frac{d\sigma^2(\mathbf{q})}{dEd\Omega} = \frac{4m_e}{na_0h^2}\sum_{i,j}\frac{q_i {\varepsilon_2}^{ij} q_j}{q^4}. \tag{3}$$

From now on, we will be only interested in the EELS which is obtained by integrating Eq. (3) over the angular range determined by the collection condition, i.e., the convergence semi-angle α_0 for a convergent beam and the collection semi-angle β_0 for the centered collection detector. This gives the partial angular integrated cross section as follows:

$$\frac{d\sigma}{dE}(\alpha_0,\beta_0,\tilde{O}) = \frac{4m_e}{na_0h^2}\sum_{i,j}\left(\int d\Omega \frac{q_iq_j}{q^4}\right){\varepsilon_2}^{ij}$$

$$= \frac{8\pi m_e}{na_0h^2k_0^2}\sum_{i,j} W_{ij}(\alpha_0,\beta_0,\tilde{O}){\varepsilon_2}^{ij}. \tag{4}$$

Here the weighting factor W_{ij} depends both on the specimen orientation $\tilde{O}$ and the experimental condition used, i.e., α_0 and β_0. In order to separate out these two effects, we have transformed the representation of **q** from the (x,y,z) orthogonal coordinate of the sample frame to the (X,Y,Z) orthogonal coordinate of the laboratory frame, with the Z axis

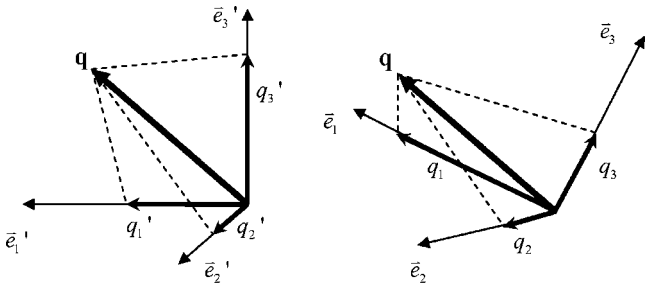

FIG. 2. The projection of the momentum transfer vector **q** in the sample frames (x,y,z) and in the laboratory frame (X,Y,Z). The components q_i (q_i') are equivalent to $\mathbf{q}\cdot\mathbf{e}_i$ $(\mathbf{q}\cdot\mathbf{e}_i')$, where the $\mathbf{e}_i$ $(\mathbf{e}_i')$ are the basis vectors of the reference frame. Two sets of components of **q** are related by the transformation matrix R whose elements are defined in terms of dot product of the basis vectors of the two reference frames.

defined to be optical axis of the electron beam. We denote the components of **q** in the (X,Y,Z) frame as q_i' (Fig. 2). Two representations of **q** are related to each other through the rotational transformation matrix **R** as:

$$q_m = \sum_i q_i' R_{mi}. \tag{5}$$

For transformation between two orthogonal coordinate systems, the rotational matrix element R_{ij} is defined to be the direction cosine between the basis vector $\mathbf{e}'$ in the (X,Y,Z) frame and the basis vector **e** in the (x,y,z) frame:[1,36]

$$R_{ij} = \mathbf{e}_i \cdot \mathbf{e}_j'. \tag{6}$$

Substituting Eq. (5) into Eq. (4), we get the expression for the weighting factor as:

$$W_{ij}(\alpha_0,\beta_0,\tilde{O}) = \frac{k_0^2}{2\pi}\sum_{m,n}\left(\int d\Omega \frac{q_m' q_n'}{q^4}\right) R_{mi}R_{nj}. \tag{7}$$

In this way we have successfully separated out the orientation factors, in the form of the product of matrix elements, from the integral within the bracket which is solely determined by the experimental setup. By inspection, we can see that the integration over the full azimuthal angle of vector **q** of the integrand with the cross-indices vanishes because of the rotational symmetry. This means that the integral has the simplified forms as follows:

$$\int d\Omega \frac{q_m' q_n'}{q^4} = \begin{cases} \displaystyle\int d\Omega \frac{q_\parallel^2}{q^4} = \frac{2\pi}{k_0^2}\xi_\parallel(\alpha_0,\beta_0) & (m=n=3) \\ \displaystyle\frac{1}{2}\int d\Omega \frac{q_\perp^2}{q^4} = \frac{2\pi}{k_0^2}\xi_\perp(\alpha_0,\beta_0) & (m=n=1 \text{ or } 2) \\ 0 & (m\neq n), \end{cases} \tag{8}$$

where we have introduced the notations $q_\parallel$ and $q_\perp$ to denote the components of **q** that are parallel and perpendicular to the incident beam direction, respectively (Fig. 1) and k_0 is the magnitude of the wave vector for the fast electron beam. The factor $2\pi/k_0^2$ is used to make the reduced integral variable $\xi_\parallel$ and $\xi_\perp$ dimensionless.

Putting the integral expression in Eq. (8) back into Eq. (7), the weighting factor can be written as:

$$W_{ij}(\alpha_0,\beta_0,\tilde{O}) = \xi_\parallel R_{3i}R_{3j} + \xi_\perp(R_{1i}R_{1j} + R_{2i}R_{2j}). \tag{9}$$

If we rearrange the product of the matrix element by applying the orthogonal property of the transformation matrix[1] as $\Sigma_m R_{mi}R_{mj} = \delta_{ij}$, and through explicit calculation using Eq. (6), we can obtain a more revealing definition for the weighting factor

$$W_{ij}(\alpha_0,\beta_0,\tilde{O}) = \xi_\perp \delta_{ij} + (\xi_\parallel - \xi_\perp)\cos\chi_i \cos\chi_j, \tag{10}$$

where the χ_i is the angle between the optical axis (the Z direction) of the laboratory frame and the ith basis vector in the sample frame. It is clear that the second term in Eq. (10) gives the information about orientation of the sample, so the magic angle condition is defined by

$$\xi_\parallel(\alpha_0^{\mathrm{MA}},\beta_0^{\mathrm{MA}}) = \xi_\perp(\alpha_0^{\mathrm{MA}},\beta_0^{\mathrm{MA}}). \tag{11}$$

Note that our derivation has not exploited any special symmetry properties of the dielectric function, for example, some specific symmetry property possessed by a crystal structure. Hence the magic angle condition is valid for all anisotropic systems, i.e., it not only applies to single crystals, but also to amorphous materials, powders, or nanostructures as long as an effective dielectric function tensor can be defined and measured.

B. Quantum mechanical theory

The dielectric function approach is very useful in treating practical problems. However, to understand the microscopic origin of the electronic transition responsible, it is better to work explicitly in terms of a quantum mechanical theory. With the widespread use of *ab initio* quantum mechanical calculation methods, proper treatment of the electronic excitation will become routine.[37–39] It is vital to know how to relate them to measurements where specimen-orientation is an additional variable.

In quantum mechanics the inelastic scattering of high energy electrons can be described adequately by the first Born approximation as:[40,41]

$$\frac{d\sigma^2(\mathbf{q})}{dEd\Omega} = \frac{4}{a_0^2}\cdot\frac{1}{q^4}|\langle f|\exp(-i\mathbf{q}\cdot\mathbf{r})|i\rangle|^2, \tag{12}$$

where a_0 is Bohr atomic radius, and vector **r** is the coordinate of the electrons in the sample, the initial and final states of which are represented by $\langle i|$ and $\langle f|$, respectively. Since we have not considered the screening of the fast electron Coulomb potential by other electrons inside the material, this expression is only applicable to core electron excitations. Because of the inverse q-dependence, electron scattering is concentrated at small angles. We can then expand the matrix element in terms of **q** and only retain the first non-zero term

which is the dipole approximation,[25] to obtain

$$\frac{d\sigma^2(\mathbf{q})}{dEd\Omega} \approx \frac{4}{a_0^2}\cdot\frac{1}{q^4}|\langle f|\ \mathbf{q}\cdot\mathbf{r})|i\rangle|^2 = \frac{4}{a_0^2}\sum_{i,j}\frac{q_i q_j}{q^4}\langle x_i\rangle\langle x_j\rangle^*. \tag{13}$$

After projecting $\mathbf{q}$ in the sample frame (x,y,z) mentioned above, one can see the connection between Eq. (13) and Eq. (4) by identifying $\mathrm{Im}(\varepsilon^{ij})$ with $\langle x_i\rangle\langle x_j\rangle^*$. The rest of the derivation can follow the procedure used in the dielectric formalism. Thus, we should arrive at the same conclusion as Eq. (7), so the magic angle condition should be the same as Eq. (11), i.e., $\xi_\parallel=\xi_\perp$.

C. The solution of the magic angle condition

The magic angle condition refers to the convergence and collection semi-angles, α_0 and β_0, respectively, which define the experimental setup where Eq. (11) is satisfied. We recall that the fast electron has the simple energy-momentum relation $E_0=\hbar^2k_0^2/2m$ so the energy-loss process must satisfy the following energy and momentum relations:

$$E = E_0 - E_f = \frac{\hbar^2(k_0^2-k_f^2)}{2m}, \tag{14}$$

$$\mathbf{q} = \mathbf{k}_0 - \mathbf{k}_f \tag{15}$$

or

$$q^2 = k_0^2 + k_f^2 - 2k_0k_f\cos\theta. \tag{16}$$

The simplest test case for magic angle conditions is for an experimental setup involving parallel beam illumination. In this case, the scattering angle involved (θ) is just the function of the semi-angle (β), defined to be the angle between the wave vector of the scattered electrons and the electron optical axis. For an axially centered circular detector, the maximum and minimum values of the momentum transfer are given by:

$$q_{min} = k_0 - k_f = k_0\theta_E, \tag{17a}$$

$$q_{max} = k_0^2 + k_f^2 - 2k_0k_f\cos\beta_0. \tag{17b}$$

Using the above expressions for q to calculate the integral, following Paxton *et al.*,[33] one obtains the result for the reduced integrals defined in Eq. (8) as:

$$\xi_\parallel = A = \frac{1}{8}\frac{2m}{\hbar^2}\frac{E^2}{E_0}\left(\frac{1}{q_{min}^2}-\frac{1}{q_{max}^2}\right)+\frac{1}{2}\frac{E}{E_0}\ln\frac{q_{max}}{q_{min}} + \frac{1}{8}\frac{\hbar^2}{2m}\frac{1}{E_0}(q_{max}^2-q_{min}^2), \tag{18a}$$

$$\xi_\perp = \frac{B-A}{2} = \frac{1}{2}\left(\ln\frac{q_{max}}{q_{min}}-\xi_\parallel\right). \tag{18b}$$

This complex solution for the parallel beam illumination can be simplified because we are interested in the small-angle region where dipole approximation holds, so we can use the small angle approximation for $q_\perp(\sim k_0\theta)$ and $q_\parallel(\sim q_{\min}=k_0\theta_E)$ to obtain a more simplified form for the reduced integrals

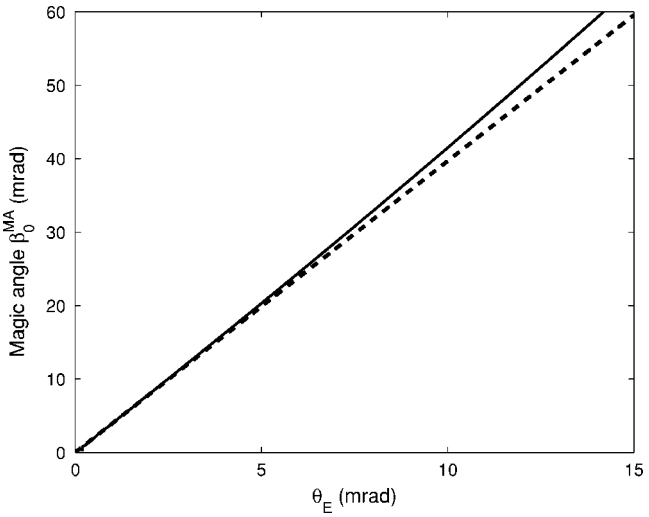

FIG. 3. The magic angle is a function of the θ_E in the parallel illumination case under the small angle approximation, i.e., $\beta_0^{\mathrm{MA}}=3.97\theta_E$ (dashed), and for cases not limited by the small angle approximation (solid), i.e., solution of Eqs. (11) and (18).

$$\xi_\parallel = A \approx \frac{\hat{\beta}_0^2}{2(\hat{\beta}_0^2+1)}, \tag{19a}$$

$$\xi_\perp = \frac{B-A}{2} \approx \frac{1}{4}\left[\ln(1+\hat{\beta}_0^2)-\frac{\hat{\beta}_0^2}{\hat{\beta}_0^2+1}\right], \tag{19b}$$

where we have used the reduced collection angle $\hat{\beta}_0=\beta_0/\theta_E$. We can solve the magic angle condition using the magic angle relation $\xi_\parallel=\xi_\perp$, i.e., $B=3A$. Within the small angle approximation, this is satisfied for $\beta_0^{\mathrm{MA}}=3.97\theta_E$, or $4\theta_E$ approximately as shown initially for a uniaxial system.[28] In Fig. 3, the magic angle solution for the parallel beam illumination setup is plotted as a function of θ_E, with and without small angle approximation. Both are very similar indeed.

D. Convergence angle effect of the magic angle condition

In many cases, explicitly for a focused probe system used for high resolution microanalysis or implicitly because of the need to increase the illumination level at the sample, a slightly convergent beam is deployed and the magic angle solution for the parallel illumination condition becomes inapplicable. To take into account the convergence effect, we need to re-examine the momentum conservation relation shown in Eq. (16). This vector relation can be decomposed according to the vector components parallel and the perpendicular to the electron optical axis. In the small-angle approximation (see Fig. 4), the parallel version of this relation is a scalar equation:

$$q_\parallel \equiv -q_Z = k_0\theta_E \tag{20}$$

and perpendicular components of $\mathbf{q}$ are defined as follows:

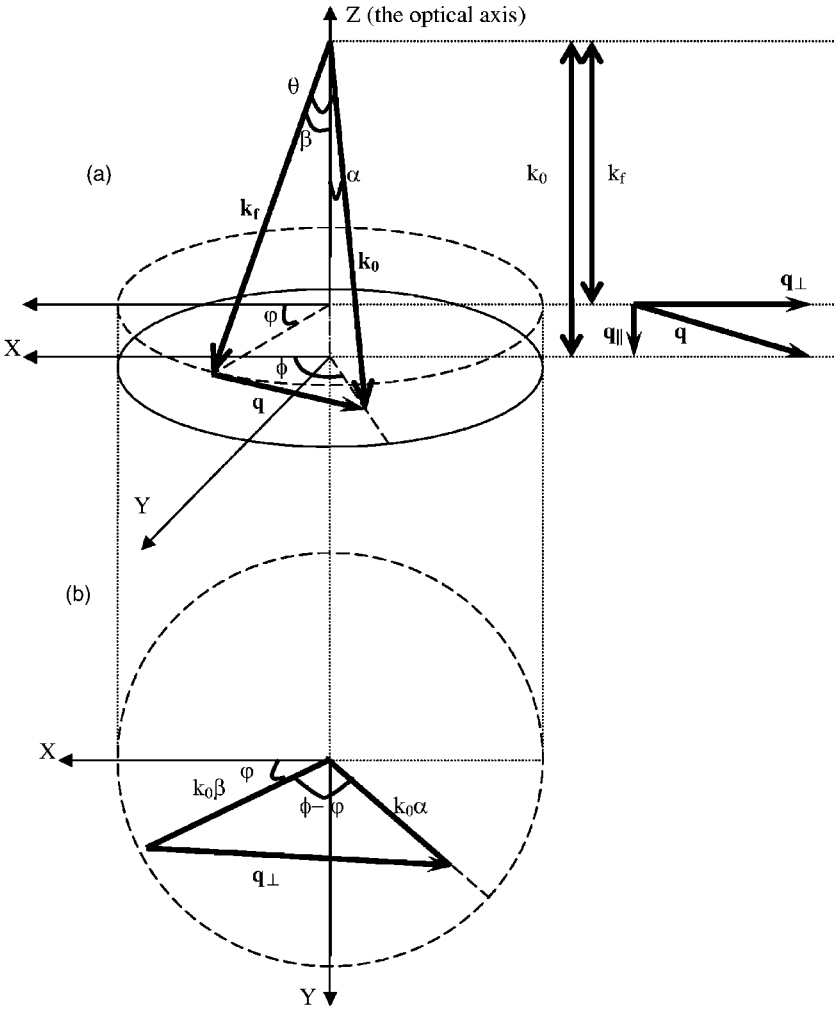

FIG. 4. Momentum vector diagram of the inelastic scattering under the small angle approximation (a) and its projection in the plane perpendicular to the optical axis (b). The convergence angle effect has been taken into consideration.

$$q_X = k_0(\alpha \cos \phi - \beta \cos \varphi)$$

$$q_Y = k_0(\alpha \sin \phi - \beta \sin \varphi) \tag{21}$$

$$q_\perp^2 = q_X^2 + q_Y^2 = k_0^2\theta^2,$$

where ϕ and φ are azimuth angles for wave vectors of the incident and scattered electrons, respectively, and θ is the scattering angle between the direction of the incident electron and that of the scattered electron. The latter is related to α (β), the angle between the incident (scattered) electron and the electron beam axis, by spherical trigonometry (see the appendix):

$$\theta^2(\alpha,\beta,\phi-\varphi) = \alpha^2 + \beta^2 - 2\alpha\beta\cos(\phi-\varphi). \tag{22}$$

Then, the reduced integral defined in Eq. (8) has the following form:

$$\xi_\parallel = A', \tag{23a}$$

$$\xi_\perp = \frac{B'-A'}{2}, \tag{23b}$$

where

$$A' = \frac{1}{2\pi^2\alpha_0^2}\int_0^{\alpha_0}\alpha d\alpha\int_0^{2\pi}d\phi\int_0^{\beta_0}\beta d\beta \times\int_0^{2\pi}d\varphi\frac{\theta_E^2}{[\theta_E^2+\theta^2(\alpha,\beta,\phi-\varphi)]^2}, \tag{24a}$$

$$B' = \frac{1}{2\pi^2\alpha_0^2}\int_0^{\alpha_0}\alpha d\alpha\int_0^{2\pi}d\phi\int_0^{\beta_0}\beta d\beta \times\int_0^{2\pi}d\varphi\frac{1}{\theta_E^2+\theta^2(\alpha,\beta,\phi-\varphi)}. \tag{24b}$$

Thus the solution of Eq. (11) is equivalent to $B'=3A'$. Equation (23) is equivalent to Eq. (19) when the convergence angle α_0 approaches zero. The numerical result is plotted as a contour in Fig. 5. Our result agrees with the result given by Souce *et al.*[19] in their determination for a uniaxial system through a more tedious integration. It is worth pointing out that an earlier prediction by Menon and Yuan[28] for the magic angle condition in the convergent beam case is incorrect because it did not perform the actual azimuthal angular integration for both the incident beam and the scattered beam.

A striking feature of the solution shown above is the symmetry, that is, the interchangeability between the beam con-

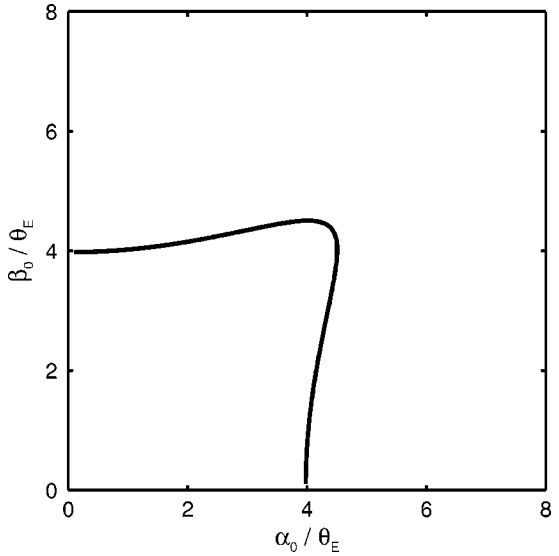

FIG. 5. The contour expression for magic angles condition in EELS of anisotropic core electron excitation.

vergence range α_0 of the incident electron and angular range β_0 of the collection of scattered electrons. This is already evident in Eq. (22). This can be traced to the small-angle approximation. Figure 4 shows that the surface of the Edward sphere described by the fast electrons becomes a plane of constant energy in the small angle approximation. It has been argued that dependence on α_0 and β_0 are not symmetrical,[28] because the interchange of α and β produces another momentum transfer vector which has the same parallel vector component but with a perpendicular component which is pointing in the opposite direction. Thus in a general case, the interchangeability of the convergence and the collection angles may not be valid. But in angular integrated spectroscopy, and in the small angle approximation, cross section depends only on the square modulus of **q** [see Eq. (8)], hence the interchangeability holds.

III. DISCUSSION

Our theoretical analysis not only gives us a definition of the magic angle conditions, valid for an arbitrary anisotropic system, but it also gives a general expression. This allows us to investigate in more detail the physical meaning of the magic angle conditions as well as understanding the discrepancy between the various reported magic angle analyses.

A. General expression of EELS cross section in anisotropic systems

A general expression can be worked out by substituting the result of Eq. (10) back into Eq. (4). This gives the cross section for the partially angular integrated electron energy-loss spectrum for core electron excitation in any anisotropic material systems in terms of their macroscopic dielectric function as:

$$\frac{d\sigma}{dE}(\alpha_0,\beta_0,\tilde{O}) = \frac{8\pi m_e}{n a_0 h^2 k_0^2}\left[\xi_\perp \,\mathrm{Im}[\mathrm{Tr}(\varepsilon)] + (\xi_\parallel - \xi_\perp)\sum_{i,j} \cos\chi_i \cos\chi_j \varepsilon_2^{ij}\right], \quad (25)$$

As the trace of the dielectric function "metric tensor" $\mathrm{Tr}(\varepsilon)$ $(=\Sigma_j \varepsilon^{ij})$ is invariant with respect to rotational transformation, the first part of the expression does not change with specimen orientation. The second part has a pre-factor that vanishes at the magic angle conditions. So the cross section for core electron excitation using MAEELS is

$$\frac{d\sigma}{dE}(\alpha_0^{\mathrm{MA}},\beta_0^{\mathrm{MA}}) = \frac{8\pi m_e}{n a_0 h^2 k_0^2}\xi_\perp^{\mathrm{MA}} \,\mathrm{Im}[\mathrm{Tr}(\varepsilon)]. \quad (26)$$

B. Physical meaning of the magic angle effect

Another way to write Eq. (25) is as follows:

$$\frac{d\sigma}{dE}(\alpha_0,\beta_0,\tilde{O}) = \frac{8\pi m_e}{n a_0 h^2 k_0^2}\left\{(\xi_\parallel + 2\xi_\perp)\frac{\mathrm{Im}[\mathrm{Tr}(\varepsilon)]}{3} + (\xi_\parallel - \xi_\perp) \times \sum_{i,j}\left(\cos\chi_i \cos\chi_j - \tfrac{1}{3}\delta_{ij}\right)\varepsilon_2^{ij}\right\}. \quad (27)$$

As before, the factor $(\xi_\parallel - \xi_\perp)$ gives the magic angle condition. However, if we rotate the crystal over all possible orientations $(\tilde{O})$, the averaged value of the angular dependent factors can be written as:[36]

$$\overline{(\cos\chi_i \cos\chi_j)} = \tfrac{1}{3}\delta_{ij}. \quad (28)$$

This means that the second term in Eq. (27) drops out when the cross section is averaged over all orientations, even if the magic angle condition is not satisfied, i.e.,

$$\frac{\overline{d\sigma}}{dE}(\alpha_0,\beta_0) = \frac{8\pi m_e}{n a_0 h^2 k_0^2}\left\{(\xi_\parallel + 2\xi_\perp)\frac{\mathrm{Im}[\mathrm{Tr}(\varepsilon)]}{3}\right\}. \quad (29)$$

Thus we demonstrated that the spectrum obtained at magic angle condition is equivalent to that obtained by orientational averaging. This reason can be explained mathematically as follows.

In normal orientational averaging, the orientation can refer either to that of the specimen or the external perturbation, i.e., the orientation of the applied field defined by the momentum transfer vector **q** in EELS. We can distinguish the averaging over the azimuth angle from 0 to 2π, from averaging over the polar angle from 0 to π. In MAEELS, the azimuth angle averaging is achieved by using an axially placed circular detector. The remaining orientational averaging of **q** over the full polar angle range is not possible to achieve in EELS experiments, but the equivalent result may be obtained by integrating over a limited range of polar angles because electron scattering is skewed toward the small angle. However, it is not always possible to find the appropriate polar angular range, hence the existence of magic angle condition is not automatically assured.

TABLE I. The predicted values of the magic collection angle for the parallel illumination case.

Authors	Zhu[11]	Menon[28]	Paxton[33]	Souche[19]	Daniels[29]
$MA_{\parallel}(\beta_0^{MA}/\theta_E)$	1.8	4	1.36	3.97	1.98

C. Comparison with other analysis

Now we can compare our prediction for the magic angle value with other derivations (see Table I) and analyze the reasons for the diversity of the predicted values.

Menon and Yuan[28] and Souche *et al.*[19] both derived their values by working out the anisotropic spectral response in a uniaxial system, but otherwise their conclusions are identical with our general result.

Most interesting is that of Paxton *et al.*,[33] who tried to derive a general theory for the magic angle condition. In their paper, the momentum transfer vector **q** is projected in the laboratory frame (X,Y,Z) defined above, so we have the quantum mechanical transitional matrix element as:

$$\begin{aligned}|\langle f|\ \mathbf{q}\cdot\mathbf{r})|i\rangle|^2 &= |\langle f|q_X X + q_Y Y + q_Z Z|i\rangle|^2 \\ &= q_X^2\langle X\rangle^2 + q_Y^2\langle Y\rangle^2 + q_Z^2\langle Z\rangle^2 + 2q_Xq_Y\,\mathrm{Re}[\langle X\rangle \\ &\quad\times\langle Y\rangle^*] \\ &\quad + 2q_Yq_Z\,\mathrm{Re}[\langle Y\rangle\langle Z\rangle^*] + 2q_Zq_X\,\mathrm{Re}[\langle Z\rangle\langle X\rangle^*],\end{aligned} \tag{30}$$

where $\langle X\rangle^2=|\langle f|X|i\rangle|^2$, and $\langle X\rangle=|\langle f|X|i\rangle|$, the $\langle Y\rangle^2$, $\langle Z\rangle^2$, $\langle Y\rangle$, and $\langle Z\rangle$ have a similar definition. As discussed above, using the weighting given in Eq. (8), the angular integrated cross section can be written as:

$$\frac{d\sigma}{dE}(\alpha_0,\beta_0,\widetilde{O}) \propto \xi_\perp\cdot(\langle X\rangle^2+\langle Y\rangle^2) + \xi_\parallel\cdot\langle Z\rangle^2. \tag{31}$$

If $\xi_\perp=\xi_\parallel=\xi_0$, then we have:

$$\frac{d\sigma}{dE}(\alpha_0^{MA},\beta_0^{MA}) \propto \xi_0\cdot(\langle X\rangle^2+\langle Y\rangle^2+\langle Z\rangle^2). \tag{32}$$

Paxton *et al.*[33] derived the magic angle condition by insisting that the isotropic spectra are given by this equation without giving detailed explanation. To show that it is orientation independent, we first consider a case where the specimen frame coincides with the laboratory frame, then

$$\langle X\rangle^2+\langle Y\rangle^2+\langle Z\rangle^2 = \langle x\rangle^2+\langle y\rangle^2+\langle z\rangle^2. \tag{33}$$

As the latter is proportional to the trace of the imaginary part of the dielectric function, it is invariable to rotation. So Paxton *et al.*[33] chose the correct magic angle condition, and should arrive at the same value for the magic angle as we do. But for reasons we could not understand, they concluded that the $MA_\parallel$ is about $1.36\theta_E$. We believe that it is a trivial mistake.

The derivation of Daniels *et al.*[29] has some similarity to our Eq. (30), but they have used the substitution in the beam direction coordinate (X,Y,Z) as:

$$\begin{aligned} q_X &= q_{XY}\cos\phi, \\ q_Y &= q_{XY}\sin\phi, \end{aligned} \tag{34}$$

$$\begin{aligned} X &= r_{XY}\cos\phi', \\ Y &= r_{XY}\sin\phi', \end{aligned} \tag{35}$$

where the r_{XY} was defined as the magnitude of vector $\mathbf{r}_{XY}$—the position vector of the sample electron in the X-Y plane where the collection detector lies, and q_{XY} has a similar definition. However, Daniels *et al.*[29] assumed that $\phi\neq\phi'$, so their subsequent calculation cannot be correct.

Zhu *et al.*[11] correctly recognized the importance of the rotationally symmetry of the experimental setup, i.e., that the cross term as shown in Eq. (8) should vanish in integrating over azimuthal angle, so they focused on estimating the weighting of the cross section along the polar angular range as:

$$\bar{q}_\parallel = \bar{q}_\perp, \tag{36}$$

where

$$\bar{q}_i = \int q_i\left(\frac{d^2\sigma}{dEd\theta}\right)d\Omega \Big/ \int\left(\frac{d^2\sigma}{dEd\theta}\right)d\Omega.$$

The normalization factor in the denominator is just the equivalent expression for the isotropic system and we can define it as N. In the small angle approximation, we have:

$$\bar{q}_\parallel = \frac{k_0}{N}\int_0^{2\pi}d\varphi\int_0^{\beta_0}\theta d\theta\frac{\theta_E}{(\theta^2+\theta_E^2)}, \tag{37a}$$

$$\bar{q}_\perp = \frac{k_0}{N}\int_0^{2\pi}d\varphi\int_0^{\beta_0}\theta d\theta\frac{\theta}{(\theta^2+\theta_E^2)}. \tag{37b}$$

In fact $q_\perp=k_0\bar{\theta}$ where $\bar{\theta}$ is the so-called mean scattering angle defined in Egerton's book,[25] and has a value $\bar{\theta}=2\theta_E(\hat{\beta}_0-\arctan\hat{\beta}_0)/\ln(\hat{\beta}_0^2+1)$, and $q_\parallel=k_0\theta_E$. For example, in his definition $\bar{\theta}=\theta_E$ and we can resolve $\beta_0^{MA}\approx 1.76\theta_E$ according to this relation. For comparison, our equivalent integrals defined in Eqs. (8) and (11) can be rewritten under the small angle approximation as

$$\xi_\parallel = \int_0^{\beta_0}\theta d\theta\frac{\theta_E^2}{(\theta^2+\theta_E^2)^2}, \tag{38a}$$

$$\xi_\perp = \frac{1}{2}\int_0^{\beta_0}\theta d\theta\frac{\theta^2}{(\theta^2+\theta_E^2)^2}. \tag{38b}$$

Thus the guess of Zhu *et al.* is incorrect numerically. By a similar argument, Gloter *et al.*[34] guessed a different weighting of transition with **q** parallel to the beam direction and estimated it with $(\mathbf{q}\cdot\mathbf{k}_0)^2/q^2{k_0}^2$. They also used the isotropic angular distribution as the normalized factor. Remarkably, their guess is correct for parallel illumination case, but their expression cannot correctly account for the convergence effect because it does not consider the scattering when the

incident and scattered electron beams are not in the same plane as the beam optical axis.

In summary, we have analyzed the reasons for the different prediction of magic angle values, and found all the discrepancies can be understood for either by the numerical mistakes or over-simplification in the derivation. Given that, a comparison between the experimental measurement and our theoretical prediction should reveal either the simplicity of the original assumptions we all share or the experimental difficulty in achieving the required conditions.

The existence of the "magic angle" effect has been experimentally demonstrated by Menon and Yuan in their 1998 paper[28] by showing that the C 1*s* absorption edge shape (which contains a strongly anisotropic core electron transition from the C 1*s* absorption edge to the anti-bonding π-dominated conduction band) is invariant of graphite specimen orientation. This is done using a convergent probe inside a scanning transmission electron microscope. Daniels et al[29] did a more systematic work and also confirmed the existence of the "magic angle" effect.

Daniels *et al.*[29] also experimentally determined that the actual value of the magic angle for collection semi-angle for C 1*s* core loss signal is 1.5–1.8 mrad for a parallel illumination by incident electrons of 200 kV, or 2.1–2.5 θ_E. If we use the relativistic expression θ_E^{rel} of Ritchie and Howie[32] to account for high energy nature of the 200 kV electrons,[42] i.e., $\theta_E^{rel} \approx 0.84$ mrad, then we have $\beta_0^{\mathrm{MA}} = 1.8-2.2\ \theta_E^{rel}$. Both estimates are different from our theoretical value. Given the above discussion, we are confident that this discrepancy cannot be accounted for by our model as some claimed. It suggests that further improvement to our model may be necessary. We can list a number of factors that might modify the prediction in our model, such as non-dipole transition,[25] the coherent scattering effect,[43] the channeling effect,[25] or the full relativistic effect.[44] However, these factors may affect the exact values of the magic angle, but not the conclusion that the magic angle effect, if it exists, applies to all anisotropic systems and that the spectra collected under the magic angle condition represent an orientation average.

One way to confirm that the spectra acquired at the magic angle are equivalent to a rotationally averaged spectrum is to compare the spectra acquired from a spherically nanoparticles with concentric shells made of grapheme layers[45] with that acquired from graphite single crystal at the magic angle conditions.[28] At the moment, this comparison is not feasible because the spectral resolutions of the existing spectra are very different.

IV. APPLICATIONS

A. "Magic" orientation in the orthogonal systems

Here we concentrate on the most commonly encountered orthogonal system where the cross term in the dielectric tensor is zero. The cross section Eq. (25) can be rearranged as:

$$\frac{d\sigma}{dE} = \frac{8\pi m_e}{na_0h^2k_0^2}\left\{\sum_j W_{jj}\varepsilon_2^{jj}\right\} = \frac{8\pi m_e}{na_0h^2k_0^2}\left\{(2\xi_\perp + \xi_\parallel)\frac{\mathrm{Im}[\mathrm{Tr}(\varepsilon)]}{3} + (\xi_\parallel - \xi_\perp)\sum_j (\cos^2\chi_j - \tfrac{1}{3})\varepsilon_2^{jj}\right\}. \quad (39)$$

Again the first part is rotationally invariant so it represents the isotropic spectrum. The second part contains information about the specimen rotation. The first bracket represents the factor responsible for the magic angle condition. The interesting point is the existence of other factors $(\cos^2\chi_j - 1/3)$ inside the summation over j. This suggests that the second part will also vanish if all the brackets within the summation sign equal to zero. They uniquely define a specific specimen orientation ($\chi_j = 54.7°$) which we may label as the "magic" orientation. Again the spectrum so obtained equals that obtained at the magic angle condition or by orientational averaging. This is understandable as $\cos\chi_j$ is the projection of the jth basis vector on the optical axis, so each principal symmetry electronic excitation contributes equally. By rotation symmetry about the beam direction, the same result holds for the more general case involving convergence illumination.

In uniaxial systems whose dielectric function has only two variables $\varepsilon_\parallel$ and $\varepsilon_\perp$, the angular integrated cross section as shown in Eq. (39) becomes

$$\frac{d\sigma}{dE} = \frac{8\pi m_e}{na_0h^2k_0^2}\left\{(2\xi_\perp + \xi_\parallel)\frac{\varepsilon_2^\parallel + 2\varepsilon_2^\perp}{3} + (\xi_\parallel - \xi_\perp) \times (\cos^2\chi_3 - \tfrac{1}{3})(\varepsilon_2^\parallel - \varepsilon_2^\perp)\right\}. \quad (40)$$

Clearly, the "magic" orientation defined above is reduced to a "magic angle" between the z axis of the sample and the optical axis, i.e., $\chi_3 = 54.7°$ in uniaxial systems. Although we may distinguish this "magic angle" of specimen orientation with the magic angle for the beam convergence and collection in both cases, the acquired spectra are again equivalent to spherically averaged spectra and hence they can be considered as a part of MAEELS family.

In summary, the "magic" orientation can provide a set up at which the spectra should be the same as the spectra gained at the magic angle for the system where the symmetry is higher than orthogonal, and this "magic" orientation will lose its meaning in a system whose dielectric function has nonzero off-diagonal elements.

Our analysis suggests that a better way to represent the anisotropic response of EELS is to write it as a linear combination of the orientationally averaged (also called "isotropic") spectrum and an orientation-dependent spectrum. In uniaxial systems, the orientation-dependent spectrum can be further expressed as a product of the magic angle factor, the magic orientation factor, and a dichroic spectrum:

$$\varepsilon_2|_{Anisotropic} = (2\xi_\perp + \xi_\parallel)\cdot\ \varepsilon_2|_{Average} + (\xi_\parallel - \xi_\perp)\left(\cos^2\chi_3 - \tfrac{1}{3}\right)\cdot\ \varepsilon_2|_{Dichroic}, \quad (41)$$

where

$$\varepsilon_2|_{Average} = \frac{2\varepsilon_2^\perp + \varepsilon_2^\parallel}{3}, \quad (42a)$$

$$\varepsilon_2|_{Dichroic} = \varepsilon_2^\parallel - \varepsilon_2^\perp. \quad (42b)$$

This formula should offer a practical way to study the anisotropy in the core electron excitation as well as encoding the magic angle and magic orientation conditions.

B. Connections between MAS for EELS, for NMR, and for XAS

The magic orientation effect has a direct analogue with the "magic angle effect" in XAS experiments and indirectly with magic angle spinning nuclear magnetic resonance (MAS-NMR).

In surface extended x-ray absorption fine structure (SEXAFS),[6,7] one can study the bonding length as well as the local coordination number of the excited atoms. However, contribution of more than one shell to the measured EXAFS can result in *a polarization dependent measured distance* from absorbing atom to the neighboring atoms and affect the effective coordination number. If there is a higher than twofold symmetry around the surface normal, the correct distance and the real coordination number can be directly measured if the angle, between the electric field vector **E** of the incident x ray and the surface normal of the single crystal, is equivalent to 54.7° exactly. This is because the system being probed is effectively an uniaxial system.

Another famous example is the MAS-NMR technique for solid.[24,46,47] If the material, whether it is a single crystal, polycrystal or power, is spun with high speed about an axis which is at 54.7° with respect to the applied magnetic field, the NMR result will be independent of the orientation of the sample. MAS-NMR is also related to the orientational magic angle effect because one is effectively using spinning to create an effective "uniaxial system" out of powdered samples.

V. CONCLUSION

We have presented a general model describing anisotropy of the core-level electron excitation in EELS measurement and have determined the magic angle condition at which the sample orientation becomes irrelevant. After comparing our derivation with reported theoretical efforts, we can explain all the reasons for disagreement in the literature predicting the value of the magic angle and show that the differences in no way invalidate our approach. Furthermore, for the first time, we show that the magic angle condition is applicable in all anisotropic systems and that the spectrum at the magic angle condition is equivalent to the rotational average of the sample. The same analysis can also give the general expression for EELS of core electron excitation in anisotropic system. In certain cases, we found the magic orientation condition in which equivalent spectral information is obtained as in MAEELS. Its relation with other "magic angle effect" is clarified. In addition, the analysis shows that EELS in a uniaxial system can be written as a sum of the effective "isotropic" spectrum and the linear dichroic spectrum. This should facilitate the study of dichroism in anisotropic systems.

ACKNOWLEDGMENTS

This research is supported by the National Key Research and Development Project for Basic Research from Ministry of Science and Technology, the Changjiang Scholar Program of Ministry of Education and the "100"-talent program of the Tsinghua University. We also thank the referees for suggestions about the test for orientationally averaged spectra in MAEELS.

APPENDIX: THE GEOMETRICAL EXPLANATION FOR EQ. (22)

The perpendicular component of the momentum transfer **q** can be seen as a sum of the perpendicular components of the initial and the final wave-vector in the case of the convergence beam as:

$$\mathbf{q}_\perp = \mathbf{k}_0^\perp - \mathbf{k}_f^\perp . \tag{A1}$$

According to the vector relations shown in Fig. 4 under the small angle approximation, we have:

$$q_\perp = k_0 \theta, \tag{A2}$$

$$k_0^\perp = k_0 \alpha, \tag{A3}$$

$$k_f^\perp = k_0 \beta. \tag{A4}$$

Thus the scattering angle θ can be written following the vector combination rule as:

$$\vec{\theta} = \vec{\alpha} - \vec{\beta}, \tag{A5}$$

where the directional properties of these angular vectors are defined to be the same as the perpendicular components of their corresponding wave vectors. According to the law of cosines, the magnitude of $\vec{\theta}$ therefore can be written as Eq. (22),

$$\theta(\alpha, \beta, \phi - \varphi)^2 = \alpha^2 + \beta^2 - 2\alpha\beta \cos(\phi - \varphi).$$

*Electronic address: yuanjun@mail.tsinghua.edu.cn

[1] H. Juretschke, *Macroscopic Physics of Anisotropic Solids* (Benjamin, Reading, MA, 1974).

[2] R. Leapman and J. Silcox, Phys. Rev. Lett. **42**, 1361 (1979).

[3] R. Leapman, P. Fejes, and J. Silcox, Phys. Rev. B **28**, 2361 (1983).

[4] M. Disko, O. Krivanek, and P. Rez, Phys. Rev. B **25**, 4252 (1982).

[5] P. Baston, Phys. Rev. B **48**, 2608 (1993).

[6] D. Kiningsberger and R. Prins, *X-ray Absorption: Principles, Applications, Techniques of EXAFS, SEXAFS and XANES* (Wiley-Interscience, New York, 1988).

[7] J. Stöhr, *NEXAFS Spectroscopy* (Springer, Berlin, 1992).
[8] Y. S. Lee, Y. Murakami, D. Shindo, and T. Oikawa, Mater. Trans., JIM **41**, 555 (2000).
[9] M. Lubbe, P. R. Bressler, W. Braun, T. U. Kampen, and D. R. T. Zahn, J. Appl. Phys. **86**, 209 (1999).
[10] Y. M. Zhu, Z. Wang, and M. Suenaga, Philos. Mag. A **67**, 11 (1993).
[11] Y. M. Zhu, J. M. Zuo, A. R. Moodenbaugh, and M. Suenaga, Philos. Mag. A **70**, 969 (1994).
[12] J. Fink, N. Nucker, E. Pellegrin, H. Romberg, M. Alexander, and M. Knupfer, J. Electron Spectrosc. Relat. Phenom. **66**, 395 (1994).
[13] N. Nucker, E. Pellegrin, P. Schweiss, J. Fink, S. Molodtsov, C. Simmons, G. Kaindl, W. Frentrup, A. Erb, and G. Muller-Vogt, Phys. Rev. B **51**, 8529 (1995).
[14] G. A. Botton, C. B. Boothroyd, and W. M. Stobbs, Ultramicroscopy **59**, 93 (1995).
[15] Y. Zhu, A. R. Moodenbaugh, G. Schneider, J. W. Davenport, T. Vogt, Q. Li, G. Gu, D. A. Fischer, and J. Tafto, Phys. Rev. Lett. **88**, 247 002 (2002).
[16] X. Kong, Y. Q. Wang, H. Li, X. F. Duan, R. C. Yu, S. C. Li, F. Y. Li, and C. Q. Jin, Appl. Phys. Lett. **80**, 778 (2002).
[17] G. P. Zhang, G. S. Chang, T. A. Callcott, D. L. Ederer, W. N. Kang, E. M. Choi, H. J. Kim, and S. I. Lee, Phys. Rev. B **67**, 174 519 (2003).
[18] R. F. Klie, H. B. Su, Y. M. Zhu, J. W. Davenport, J. C. Idrobo, N. D. Browning, and P. D. Nellist, Phys. Rev. B **67**, 144 508 (2003).
[19] C. Souche, B. Jouffrey, and M. Nelhiebel, Micron **29**, 419 (1998).
[20] O. Stephen, P. Ajayan, C. Colliex, F. Cylor-Lackmann, and E. Sandre, Phys. Rev. B **53**, 13 824 (1996).
[21] N. Vast, L. Reining, V. Olevano, P. Schattschneider, and B. Jouffrey, Phys. Rev. Lett. **88**, 037 601 (2002).
[22] A. G. T. Ruiter, J. A. Veerman, M. F. Garcia-Parajo, and N. F. van Hulst, J. Phys. Chem. A **101**, 7318 (1997).
[23] N. F. van Hulst, J. A. Veerman, M. F. Garcia-Parajo, and L. Kuipers, J. Chem. Phys. **112**, 7799 (2000).
[24] A. Rahman, *Nuclear Magnetic Resonance: Basic Principles* (Springer, New York, 1986).
[25] R. Egerton, *Electron Energy Loss Spectroscopy in the Electron Microscope* (Plenum, New York, 1996).
[26] N. Browning, J. Yuan, and L. M. Brown, Ultramicroscopy **38**, 291 (1991).
[27] N. Browning, J. Yuan, and L. M. Brown, Philos. Mag. A **67**, 261 (1993).
[28] N. K. Menon and J. Yuan, Ultramicroscopy **74**, 83 (1998).
[29] H. Daniels, A. Brown, A. Scott, T. Nichells, B. Rand, and R. Brydson, Ultramicroscopy **96**, 523 (2003).
[30] H. Kurata, K. Ishizuka, T. Kobayashi, and S. Isoda, Synth. Met. **22**, 337 (1988).
[31] H. Kurata, T. Kobayashi, and S. Isoda, Bull. Inst. Chem. Res., Kyoto Univ. **71**, 212 (1993).
[32] R. H. Ritchie and A. Howie, Philos. Mag. **36**, 463 (1977).
[33] A. T. Paxton, M. van Schilfgaarde, M. MacKenzie, and A. J. Craven, J. Phys.: Condens. Matter **12**, 729 (2000).
[34] A. Gloter, J. Ingrin, D. Bouchet, and C. Colliex, Phys. Rev. B **61**, 2587 (2000).
[35] J. Jackson, *Classical Electrodynamics* (Wiley, New York, 1984).
[36] E. Prince, *Mathematical Techniques in Crystallography and Material Science* (Springer, Berlin, 1994).
[37] M. Nelhiebel, P. H. Louf, P. Schattschneider, P. Blaha, K. Schwarz, and B. Jouffrey, Phys. Rev. B **59**, 12 807 (1999).
[38] C. Hebert-Souche, P. H. Louf, P. Blaha, M. Nelheibel, J. Luitz, P. Schattschneider, K. Schwarz, and B. Jouffrey, Ultramicroscopy **83**, 9 (2000).
[39] P. Schattschneider, C. Hebert, and B. Jouffrey, Ultramicroscopy **86**, 343 (2001).
[40] H. Bethe, *Intermediate Quantum Mechanics* (Benjamin, New York, 1964), 1st ed.
[41] M. Inokuti, Rev. Mod. Phys. **43**, 297 (1971).
[42] H. Kurata, P. Wahlbring, S. Isoda, and T. Kobayashi, Micron **28**, 381 (1997).
[43] N. K. Menon and J. Yuan, Ultramicroscopy **78**, 185 (1999).
[44] U. Fano, Phys. Rev. **102**, 385 (1956).
[45] T. Pichler, M. Knupfer, M. Golden, J. Fink, and T. Cabioc'h, Phys. Rev. B **63**, 155 415 (2001).
[46] E. Andrew, A. Bradbury, and R. Eades, Nature (London) **183**, 1802 (1959).
[47] I. Lowe, Phys. Rev. Lett. **2**, 285 (1959).